

Experimental generation of a cw cold CH₃CN molecular beam by a low-pass energy filtering

Yang Liu, Min Yun, Yong Xia, Lianzhong Deng and Jianping Yin*

Received 13th July 2009, Accepted 23rd October 2009

First published as an Advance Article on the web 25th November 2009

DOI: 10.1039/b913929j

We generate a continuous-wave (cw) cold methyl cyanide (CH₃CN) beam by using an L-shaped bent quadrupole electrostatic guide (*i.e.*, by a low-pass energy or velocity filtering), and use a photo-ionized time-of-flight mass-spectrometer method to experimentally measure and study the dependences of the longitudinal and transverse temperatures of the guided CH₃CN beam and its guiding efficiency on the guiding voltage. We find a new scaling law: the longitudinal and transverse temperatures (T_z, T_ρ) of the guided CH₃CN beam are proportional to the guiding voltage ($T_z, T_\rho \propto V_{\text{guide}}$), and further verify another scaling law: the molecular guiding efficiency η is proportional to the square of the guiding voltage ($\eta \propto V_{\text{guide}}^2$). We also obtain some simulated results consistent with our experimental ones. We also measure the divergent angle of the output molecular beam and study its dependence on the guiding voltage. Our study shows that when the guiding voltage is $V_{\text{guide}} = \pm 1$ kV, a cw cold CH₃CN beam with a longitudinal temperature of ~ 500 mK and a transverse one of ~ 40 mK can be generated by our L-shaped electrostatic guide. The divergent angle of the output CH₃CN beam is about 16.4° as $V_{\text{guide}} = \pm 4$ kV. It is clear that such a resulting cold molecular beam has some important applications in the fields of cold molecular physics, physical chemistry and chemical physics, *etc.*

1. Introduction

In the past several years there has been an explosion of research in cold molecules.¹ Compared to cold atoms, cold molecules (especially cold polar molecules) have strong chemical reactivities. Therefore, cold molecules offer many unique properties which are not available for cold atoms, such as cold or ultracold chemistry, cold molecular physics and cold molecular collisions, *etc.* Cooling molecules into the cold or ultracold regimes will push molecular spectroscopy to the fundamental level where vibrational relaxation can be directly revealed, and extremely weak interactions can be investigated. Precision molecular spectroscopy² and long interrogation times offered by cold molecules (especially in external fields) are critical to performing precision measurements, such as searching for the permanent electron electric dipole moment (EDM)³ and improving the values of fundamental constants,⁴ even pursuing the molecular optical clock.⁵ Further, there has been a proposed application in quantum computing and quantum information processing⁶ with ultracold polar molecules. The long range and anisotropic characteristics of the dipole–dipole interaction in cold polar molecules is also expected to develop new physics such as ultracold molecular collisions⁷ and cold or ultracold chemistry.⁸ Since there is so much intense, and still rapidly growing, interest in cold molecules, the generation of a cold molecular beam has become one of the hottest areas of research in the scientific explorations of cold molecules, and the resulting cold

molecules have vast numbers of applications in the fields of cold molecular physics, physics chemistry and chemical physics, *etc.*

In recent years, a variety of techniques have been developed to produce a cw or pulsed cold molecular beam, such as slowing a molecular beam with a rapid rotator,⁹ decelerating a supersonic polar-molecular beam using a time-varying electrostatic field,¹⁰ filtering an effusive beam^{11,12} by using a bent guide, producing a cold effusive beam with a 5–10 K temperature by buffer gas cooling,¹³ Zeeman decelerating a supersonic paramagnetic-molecular beam with a time-varying magnetic field,¹⁴ optical stark decelerating for a supersonic beam^{15,16} or a cw molecular beam,¹⁷ and so on. In particular, the low-pass energy (or velocity) filtering offers the simplest and most convenient method of generating a cold molecular beam by directly selecting slow and cold molecules from an effusive thermal beam, and it can be used to easily control the output flux and longitudinal temperature of the generated cold molecular beam by changing the guiding voltage. In outer space, methyl cyanide (CH₃CN) is a typical large nitrogen-bearing species which locates near hot cores and has thus become an important hot core tracer for exploring the formation of massive stars for many years by measuring its rotational transition lines. According to the relative intensities of these transitions we can deduce the temperature and density of the hot core.¹⁸ Due to this important role of CH₃CN in astrochemistry and stellar physics, it is worthwhile to cool it into the cold or ultracold regime. It is also a highly reactive organic compound, so it will be interesting to study its reactive behavior at ultracold temperatures.⁸ In addition, it is a textbook example of a prolate symmetric top featuring a large dipole moment (3.91 Debye),¹⁹ and can be easily controlled by using a relatively low electrostatic field. Therefore, it would be

State Key Laboratory of Precision Spectroscopy, Department of Physics, East China Normal University, Shanghai 200062, P. R. China. E-mail: jpyin@phy.ecnu.edu.cn

interesting and worthwhile to generate a cw cold CH_3CN beam by using a bent quadrupole electrostatic field with a lower guiding voltage.

More recently, we demonstrated an electrostatic surface and quadrupole-like guiding for cold polar molecules by using a straight hollow electrostatic field and obtain a high guiding efficiency (about 30–50%).^{20,21} In this paper, we use an L-shaped bent electrostatic guiding scheme to produce a cw cold CH_3CN beam and study the dependences of the characteristic parameters of the guided CH_3CN beam on the guiding voltage, and obtain some new and interesting experimental results. In section II, an L-shaped, bent electrostatic guiding scheme is presented. In section III, we study the dependences of the longitudinal and transverse temperatures of the cold molecular beam and its guiding efficiency on the guiding voltage, the results of which show an excellent agreement with our simulations. We also measure the divergent angle of the output molecular beam, and study the dependence of the divergent angle on the guiding voltage. In section IV, we compare our work and results with those of other groups, and sum up our new findings and results in this research. Some main results and conclusions are summarized in the final section.

2. Electrostatic bent guiding scheme

Fig. 1 shows our experimental setup to generate a cw cold CH_3CN beam by using a quadrupole electric field, which is formed by four L-shaped quadrupole electrodes with a 3 mm diameter and a 1 mm gap between two neighboring electrodes, which carry voltages of the same magnitude but of opposite polarity (hereafter we call them the guiding voltages V_{guide}). In the experiment, the sample gas in a gas reservoir is jetted from a thin ceramic nozzle, and a cw molecular beam is formed and injected into the electrostatic guiding tube at the inlet of our first section of L-shaped electrode in the first ultra-high vacuum chamber. The pressure in the gas reservoir can be flexibly adjusted from 10^{-1} Pa to 300 Pa by tuning the Swagelok low-flow metering valve (SS-SS4-VH). It should be noted that since the diameter and length of our nozzle are 0.6 mm and 1.0 mm, respectively, and our actually used reservoir pressure in the experiment is between 10 Pa and 60 Pa, the generated molecular beam is not an ideal effusion one in our experiment. The curvature radius at the bend of the L-shaped wires is $R = 12.5$ mm. As the existence of spatial quadrupole electric field, the molecules with kinetic energies larger than their Stark energies will escape from the effective guiding region and be pumped out, while the molecules with kinetic energies lower than their Stark energies will be guided along the electrodes and be detected by our home-made time-of-flight (TOF) mass spectrometer (TOFMS). So our L-shaped guiding system, as a low-pass energy (or velocity) filter, can be used to generate a cw cold molecular beam. The spatial electrostatic field distribution is calculated by using a finite element software, and the corresponding contour map when $V_{\text{guide}} = 7$ kV is shown in Fig. 1. Our calculation shows that the resulting electrostatic field is a quadrupole field distribution with a zero central E -field value, which is a hollow electrostatic tube (see Fig. 1) and can be used to guide cold polar molecules in the weak-field-seeking (WFS) states.

As shown in Fig. 1, for the sake of convenient installation, our bent quadrupole electrostatic guiding system is composed of a section of L-shaped stainless-steel quadrupole electrodes with a length of $L_1 = 35.86$ cm and another section of straight stainless-steel quadrupole electrodes with a length of $L_2 = 45$ cm (and the total length is $L_1 + L_2 = 80.86$ cm), and the gap between two sections of the quadrupole electrodes is about 1 mm. The pressures in the two vacuum chambers (chamber A and chamber B) are about 10^{-5} Pa and $\sim 10^{-7}$ Pa, respectively, which are maintained by a turbomolecular pump (KYKY, FF200-200/600C) and a sputtering ion pump (JJJ Vac, SP-400A). In the detection chamber B, the guided molecules are ionized by a pulsed and tightly focused laser beam, and detected by our homemade (Wiley-McLaren type) time-of-flight (TOF) mass spectrometer. The output signals from the multiple-channel plate (MCP) are collected and averaged on an oscilloscope (Agilent DSO3202A, 200 MHz), and are transferred to the personal computer for signal storage and processing. In our experiment, the used ionization laser is a pulsed 266 nm frequency-quadrupled Nd:YAG laser (Continuum Surelite II-10) with a single pulse energy of 10.5 mJ. Because we have no a quadrupole mass spectrometer (QMS) at present, and cannot use the so-called (or a conventional) QMS method¹¹ to measure the longitudinal velocity distribution (*i.e.*, longitudinal temperature) of the output cold molecular beam. In order to roughly estimate the longitudinal temperature of the output cold molecular beam, however, we use a pulsed high-voltage operating mode and the time-of-flight mass spectrometer (TOFMS) method to measure the longitudinal velocity distribution of the output molecular beam. It should be noted that this TOFMS method is an approximately testing one because a faster molecule that enters the guide later may catch up to a slow molecule that enters earlier during the guide is switched on, and may result in an widening for the low velocity wing of the longitudinal velocity distribution of the output cold molecular beam. This shows that the measured longitudinal temperature of cold molecular beam may be slightly higher than its real temperature. In other words, the TOFMS method is a conservatively testing one for the longitudinal temperature of a cw cold molecular beam and the real beam will be colder than one estimated by the TOFMS method.

In the experiment, all the high voltages on the guiding electrodes are delivered by four high voltage power supplies, in which two power supplies, connected to the first-section quadrupole electrodes with a length L_1 , are triggered by two fast high-voltage switches (Behlke, HTS 201-03-GSM), and the working principle of HV pulses and their circuits are similar to that in ref. 22. When the resistance between the voltage supply and the electrodes is 3 k Ω and the guiding voltages are ± 8 kV, the rising and dropping times of our HV switch circuit are about 450 ns, which is short enough to fast switch on and off the HV on the electrodes so as to measure the longitudinal velocity distribution of the output molecular beam.

Before this experiment, we calculate the Stark shifts of rotational energy levels of CH_3CN in the guiding electric field and their populations at $T = 300$ K, and simulate the movement of the guided molecules and trace their trajectories

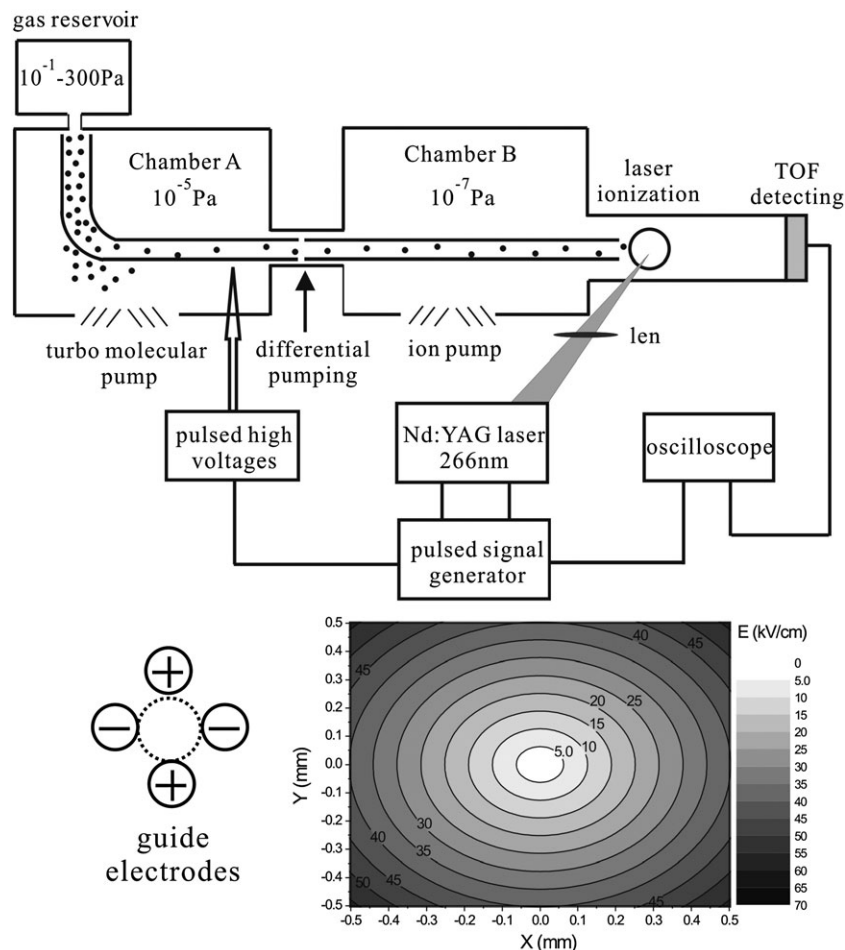


Fig. 1 Our experimental setup to generate a cold CH_3CN beam by using a bent electrostatic quadrupole guide. Inset is an array of the electrodes. The dotted circle at the center of the four electrodes shows a guiding region. The contour distribution of the electric field in the effective guiding region ($r \leq r_0$) is also shown.

in the bent electrostatic tube by using a home-made C++ program, and the corresponding details and results can be found in ref. 23. In this paper, we only show some comparisons of our simulated results with the corresponding experimental ones, which will be shown and discussed in section 3.

3. Experimental study and results

In this experiment, we generate a cw cold CH_3CN beam by using a bent quadrupole electrostatic guide, and use the TOFMS method to measure the longitudinal velocity distribution of the output cw cold molecular beam, and study the dependences of the longitudinal and transverse temperatures of the output molecular beam and its guiding efficiency on the guiding voltage, which will be reported below, respectively.

3.1 Experimental method to detect molecular velocity distributions

In recent years, Rempe's group used the QMS method to extract the longitudinal velocity distribution of a cw molecular beam by analyzing the rise time of the molecular signal after the guide is turned on.¹¹ Here we use the TOFMS method to

measure the longitudinal velocity distribution of a cw cold CH_3CN molecular beam, and the corresponding scheme of the time sequence control and synchronization for our trigger signal, HV switch, ionization laser (fire and Q-switch) and oscilloscope signal is shown Fig. 2. In order to obtain the longitudinal velocity distribution, we measure the number of cold molecules at different velocity groups, thus obtaining the dependence of the guided molecular number on the longitudinal velocity. In our experiment, the electrodes of the first section of quadrupole guide are applied on the pulsed positive and negative voltages by using two high-voltage (HV) switches, whose frequencies are the same as that of the laser (10 Hz or 20 Hz), while the voltages applied on the second section of quadrupole guide are kept to be unchanged during the whole measurement process. When the HV is switched on, the molecules start to be guided. The pulse width W_1 is the transit time of the guided molecules with a specific velocity group ($v = L_1/W_1$) from the inlet of the first section of the L-shaped guide to its outlet, while the time delay between the HV switch and the output of laser (Q-switch) corresponds to the time of flight from the inlet of molecular guiding to the position of laser ionization. So by adjusting the pulse width W_1 , we can obtain the longitudinal velocity distribution of the

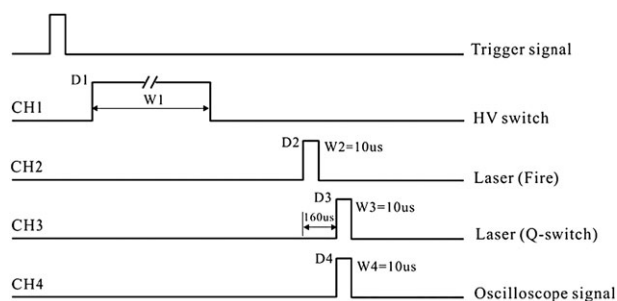


Fig. 2 Scheme of the time sequence control and synchronization for triggering signal, HV-switches, ionization laser (fire and Q-switch) and data acquisition of oscilloscope.

guided molecular beam. Also, we can measure the transversal velocity distribution of the guided molecular beam by moving the ionization position transversally.

3.2 Temperature of the output molecular beam and its guiding efficiency

In our experiment, we first measure the transverse and longitudinal velocity distributions of the output cold CH_3CN molecular beam. The CH_3CN molecule has three kinds of chemical bond, which are C–H, C–C and $\text{C}\equiv\text{N}$, and the corresponding binding energies are 4.2 eV, 5.37 eV and 9.07 eV, respectively. The energy of signal photon from a frequency-quadrupled YAG laser (266 nm, $10^{10} \text{ W cm}^{-2}$) is 4.66 eV. All of the chemical bonds may be broken by the multiphoton ionization process, so we can obtain a series of atomic or molecular ions, such as H^+ , C^+ , CH^+ , CH_2^+ , CN^+ , C_2H_3^+ , $\text{C}-\text{C}^+$, *etc.* Fig. 3 shows the typical TOF ion signals from CH_3CN molecules. Since the detected ion signal is proportional to the number N of the guided molecules, the ion signals will show the relative guiding efficiency of our guiding system. By integrating the intensity distribution of the characteristic peak CN^+ (or all of the peaks), we obtain the longitudinal velocity distribution of the guided cold CH_3CN beam, as shown in Fig. 4(a). The solid line in Fig. 4(a) shows the longitudinal velocity distribution of output cold molecular beam, which is described by:¹¹

$$P(v_z) = \frac{2v_z}{\alpha_z^2} e^{-v_z^2/\alpha_z^2}. \quad (1)$$

with $\alpha_z = \sqrt{2k_B T_z/m}$. Similarly, we can obtain the transversal velocity distribution of the output CH_3CN beam by moving the ionization position transversally, and the results are shown in Fig. 4(b). The solid line in Fig. 4(b) represents the transverse velocity distribution of the guided molecules, which is given by:¹¹

$$P(v_\rho) = \frac{1}{\alpha_\rho \sqrt{\pi}} e^{-v_\rho^2/\alpha_\rho^2} (|v_\rho| < |v_{\max}|), \quad (2)$$

where $\alpha_\rho = \sqrt{2k_B T_\rho/m}$ is the mean square root velocity, the transverse velocity is $v_\rho = \sqrt{v_x^2 + v_y^2}$, and the maximum transverse caught velocity is v_{\max} , which depends on the transverse Stark trapping potential for CH_3CN molecules in our electrostatic guiding field.

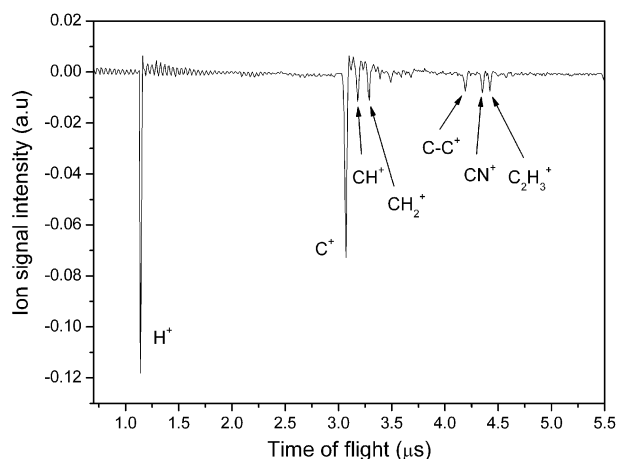


Fig. 3 TOF mass spectrum from the ionized CH_3CN molecules by a frequency-quadrupled YAG laser (266 nm, $10^{10} \text{ W cm}^{-2}$).

To make the comparison with our experimental results, we perform a Monte-Carlo simulation by using Newton's motional equation. Due to the Stark effect, the CH_3CN molecules moving in the electrostatic tube undergo a dipole gradient force and satisfy the Newton's motional equation as follows:

$$\vec{F} = -\nabla(W_{\text{Stark}}(\vec{r})) = m \frac{d^2 \vec{r}}{dt^2}, \quad (3)$$

where m is the mass of sample molecule and $W(\vec{r})$ is the Stark potential for the guided molecules in the electrostatic field. For a guided CH_3CN molecule in the WFS states, from the perturbation theory, its Stark potential in the relatively weak external field can be given by:

$$W_{\text{Stark}}(\vec{r}) = -\mu |E(\vec{r})| \left\{ \frac{MK}{J(J+1)} + \frac{\mu^2 |E(\vec{r})|^2}{2hB} \right. \\ \left. \cdot \left\{ \frac{(J^2 - K^2)(J^2 - M^2)}{J^3(2J-1)(2J+1)} \right. \right. \\ \left. \left. - \frac{[(J+1)^2 - K^2][(J+1)^2 - M^2]}{(J+1)^3(2J+1)(2J+3)} \right\} \right\} \quad (4)$$

where J is the rotational quantum number, K is the projection of J on the molecule's symmetry axis, and M is the projection of J on the external electric field $E(\vec{r})$, which is calculated using finite element software, and μ and h denote the electric dipole moment of the polar molecule and the Planck constant, respectively. However, because the perturbation theory to 2nd order is only effective for the electric field less than tens of kV cm^{-1} , the Stark shifts of the guided molecule in a relatively stronger field can be calculated numerically by diagonalizing the appropriate Hamiltonian on a sufficiently large basis set.^{24,25}

From eqn (3) and (4) or the numerical calculation method,^{24,25} we can calculate the Stark shifts of all rotational levels of CH_3CN in the guiding field and do Monte-Carlo simulations for the guided CH_3CN molecules. In our simulation, the number of the simulated molecules is generally 10^7 , and the considered Stark levels are all the WFS states $J \leq 10$

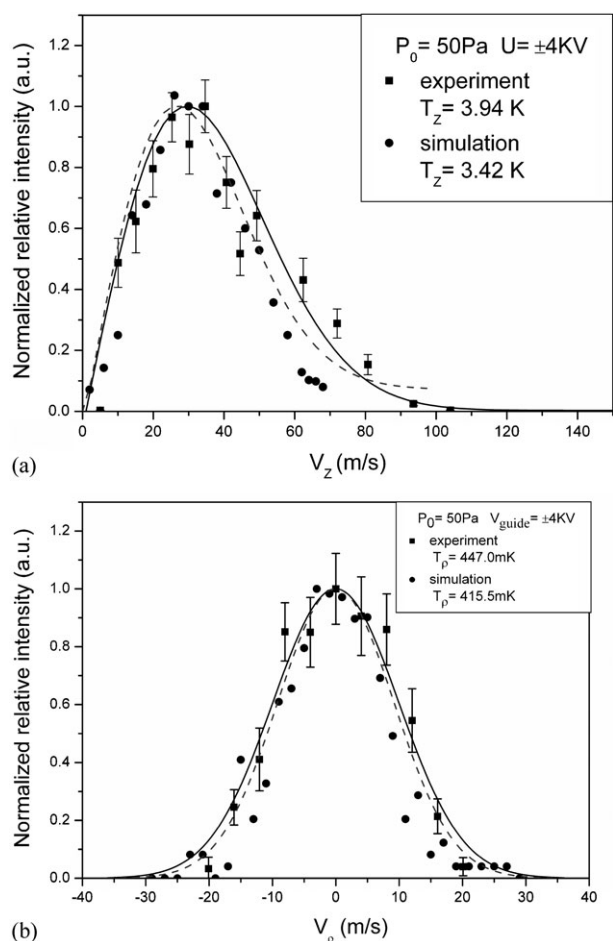


Fig. 4 (a) Longitudinal and (b) transversal velocity distributions of the output CH_3CN beam for $P_0 = 50P_a$ and $V_{\text{guide}} = 4$ kV. Squares with an error bar are the experimental data and circles are the simulated results. The solid lines and dotted ones are the fitted curves by eqn (1) and (2), respectively.

at $T = 300$ K, and the corresponding details on the partial calculations of Stark shifts of rotational levels of the CH_3CN molecule in the relatively weak field and their populations as well as on the definition and treatment of the representative states can be found in our previous theoretical work.²³ The transverse and longitudinal temperatures (including the internal vibration and rotational temperatures) of our incident CH_3CN molecular beam are 300 K. We assume that the initial spatial distribution of the simulated molecular beam at the incident plane satisfies a Gaussian distribution, and the initial longitudinal (or transverse) velocity distribution of the incident molecular beam with a temperature of 300 K satisfies a Maxwell-Boltzmann (or Gaussian) velocity distribution. The simulation of molecules in each WFS representative state with their initial velocities and positions in Cartesian coordinates start off from the inlet of our electrostatic bent guide and end at its outlet, where the velocities and positions of the guided molecules are recorded. The initial molecular number in each representative state is weighted by their populations, and at the outlet, all the guided molecular number are summed for all weighted representative states, and then the transverse, longitudinal

velocity distributions and its guiding efficiency will be obtained, respectively.

The corresponding Monte-Carlo simulated results (black circles) are shown in Fig. 4. We can see from Fig. 4 that when $P_0 = 50P_a$ and $V_{\text{guide}} = 4.0$ kV, the longitudinal and transversal temperatures of the output CH_3CN beam are $T_z = 3.94$ K and $T_\rho = 447$ mK, respectively, and our experimental results are basically consistent with our simulated ones. We can also estimate the guiding efficiency η of our system to be 4.4×10^{-5} when $P_0 = 50P_a$ and $V_{\text{guide}} = 4.0$ kV.

Afterwards, we study the dependences of output molecular-beam temperature and guiding efficiency on the guiding voltage. Fig. 5 shows the longitudinal and transversal velocity distributions of the guided CH_3CN beam for different guiding voltages. It is clear from Fig. 5 that the relative intensity of the guided CH_3CN molecules and the width of the velocity distribution are increased with increasing guiding voltage. That is to say, the guided molecular number (*i.e.*, the guiding efficiency) and its temperatures are increased with increasing guiding voltage. It is easy to understand, as the maximum cut-off velocity (molecules with a velocity exceeding it will not be guided) will be increased with increasing electric field strength (*viz.* the guiding voltage), the number of guidable molecules will be increased, and a wider velocity distribution (*i.e.*, higher temperature) will be obtained. From Fig. 5(a) and (b), we obtain the dependences of the longitudinal and transverse temperatures of the output CH_3CN beam and its guide efficiency on the guiding voltages, as shown in Fig. 6. We can see from Fig. 6 that the longitudinal and transversal temperatures (T_z, T_ρ) of the output CH_3CN beam are proportional to the guiding voltage (*i.e.*, $T_z, T_\rho \propto V_{\text{guide}}$), and the corresponding guiding efficiency η is proportional to the square of the guiding voltage (*i.e.*, $\eta \propto V_{\text{guide}}^2$), which was first found in the experiment by Rempe's group²⁶ in 2004, but they didn't clearly summarize it as a scaling law. In particular, when $V_{\text{guide}} = 1$ kV, we obtain $T_\rho = 42.3$ mK and $T_z = 520$ mK. This shows that by using our bent quadrupole electrostatic guide, we can generate a cw cold CH_3CN beam with a transverse temperature of ~ 40 mK and a longitudinal temperature of ~ 500 mK, which is slightly lower than one (~ 1 K) of a cw cold D_2O molecular beam.²⁷ From Fig. 6, we can also find that our simulated results are in good agreement with our experimental ones, and theoretically further verify the above two scaling laws.

3.3 Divergent angle of cold molecular beam

The divergent angle is another important parameter of cold molecular beam. If we measure two sets of the transversal distributions of the output cold molecular beam at two different axial positions, we can obtain the divergent angle of the output molecular beam. The measurement principle is described as follows: we take full width at $1/e$ of the maximum intensity of the measured transverse distribution as an effective diameter of the guided molecular beam, and assuming two effective diameters of the guided molecular beam at the two different axial positions are ΔX_1 and ΔX_2 , respectively, and the distance between the two axial positions is L , then the

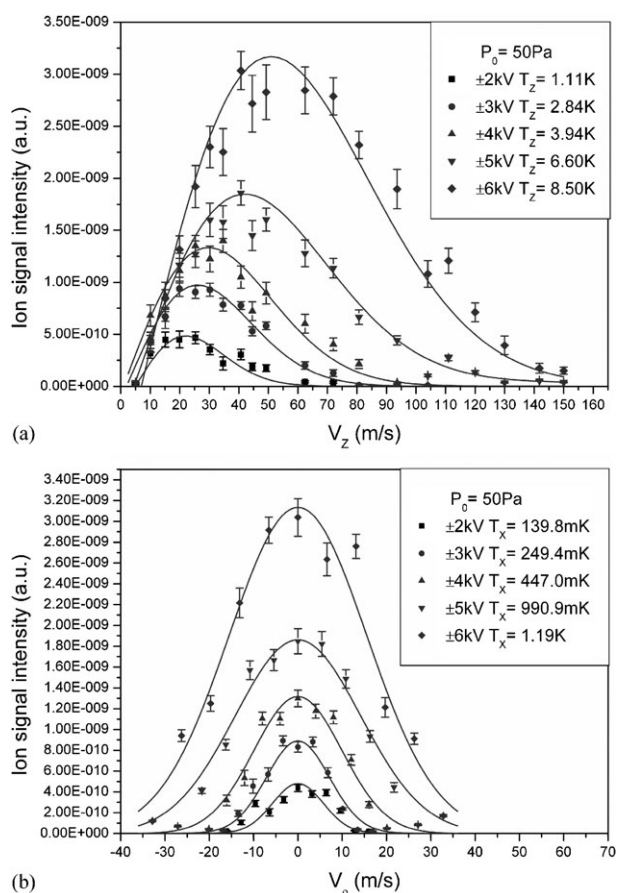


Fig. 5 Distributions of the (a) longitudinal and (b) transversal velocities of the output CH_3CN beam for $P_0 = 50P_a$ and $V_{\text{guide}} = 2, 3, 4, 5$ and 6 kV, respectively. The data points with an error bar are the experimental measured results and the solid lines are the fitted curves by eqn (2).

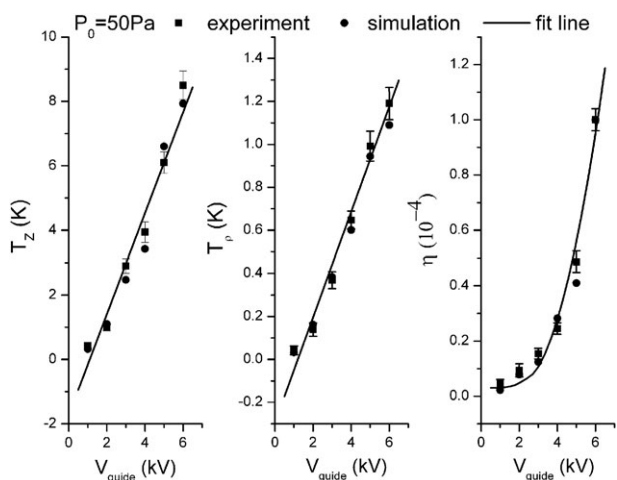


Fig. 6 Dependences of the longitudinal and transverse temperatures of the output CH_3CN beam and its guiding efficiency on the guiding voltage for $P_0 = 50P_a$. The squares with an error bar are the experimental data and the circles are the simulated results and the solid lines are the fitted curves.

divergent angle of the output cold molecular beam can be defined as $\theta = \arctan(\Delta X_2 - \Delta X_1)/(2L)$. In this experiment,

the first axial position is close to the exit of guide, and the other is far away from the exit of guide, and the distance between the two axial positions is $L = 10$ mm, which is only limited by the diameter of detecting quartz window. We measure the divergent angle of our output cold CH_3CN beam, and the results are shown in Fig. 7(a). When the guide voltage is ± 4 kV, we obtain $\Delta X_1 = 7.862$ mm and $\Delta X_2 = 11.888$ mm, then the divergent angle is estimated as $\theta = 16.38^\circ$. Alternatively, the divergent angle can be estimated from the longitudinal and transversal root-mean-square (rms) velocities of the output molecular beam. Assuming the longitudinal and transversal rms velocities are v'_z and v'_ρ respectively, then the divergent angle can be estimated by $\theta' = \arctan(v'_\rho/v'_z)$. From our experimental results, we obtain $\theta' = \arctan(14.2/44.8) = 17.4^\circ$, which is about consistent with our measured data (16.38°). In addition, we study the dependence of the divergent angle on the guiding voltage, and the results are shown in Fig. 7(b). We can find from Fig. 7(b) that when the guide voltage is equal to or lower than 4.0 kV, the beam divergent angle decreases exponentially with increasing guiding voltage. This because with the increase of the guiding voltage and when $V_{\text{guide}} \leq 4$ kV, the longitudinal filtering effect of our bent guide become a dominant one, so the increase of v'_ρ is smaller than one of v'_z with increasing guided voltage, which will result in the exponential reduction of the divergent angle with the guiding voltage. However, when the guiding voltage is further increased and larger than 4.0 kV, the divergent angle will tend to be a constant value. This because with the increase of the guiding voltage and when $V_{\text{guide}} > 4$ kV, the transversal filtering effect will be fast increased to be about the longitudinal filtering one, that is, v'_ρ is fast increased to be about equal to v'_z so that v'_ρ/v'_z tends to be a constant, which will lead to the divergent angle of output molecular beam becomes a constant value.

4. Comparison of our work and results with other groups

More recently, Softley's group used the nearly same scheme to generate the same cw cold CH_3CN beam, but used a different measurement (*i.e.*, QMS) method to study the characteristics of the resulting cold molecular beam.²⁸ Obviously, it would be better to compare our research and results with previously reported work on the velocity filtering of CH_3CN .²⁸ First, Softley's group obtained a cold CH_3CN beam with a longitudinal temperature of ~ 2 K at a guiding voltage of ± 4 kV in 2009,²⁸ which is slightly lower than ours (~ 3 K) at the same voltage ± 4 kV. This may be because our gas-source pressure and incident beam property are different from theirs. Secondly, due to a different experimental aim, they didn't use a lower guiding voltage to generate a colder molecular beam, but we used a lower voltage of ± 1 kV to generate a colder CH_3CN beam with a longitudinal temperature of ~ 0.5 K. Thirdly, to compare the translational energy distribution for the guided molecules at a guiding voltage of ± 4 kV as shown in Fig. 2 in ref. 28, we transform the longitudinal velocity of our CH_3CN beam as shown in Fig. 4(a) to the translational energy distribution, and obtain a translational energy distribution at a gas-source pressure of

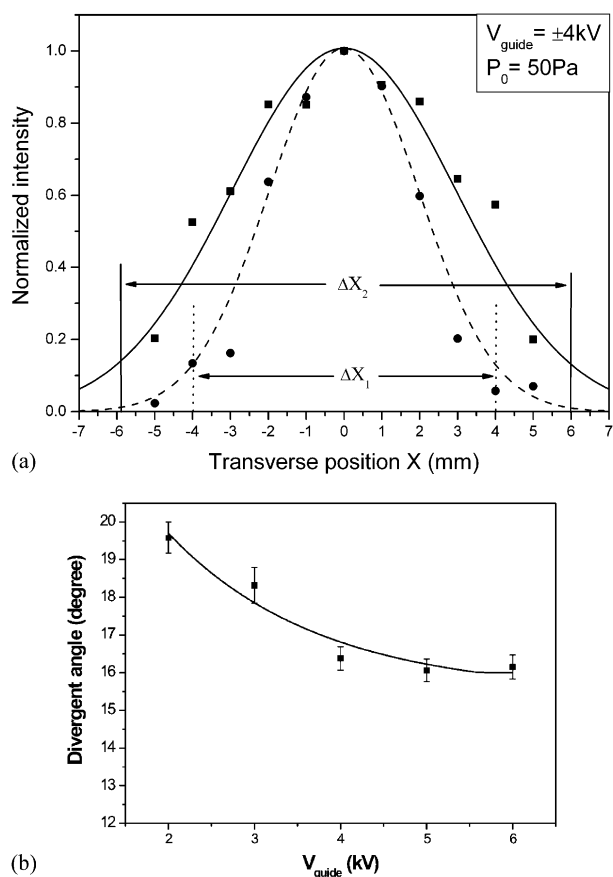


Fig. 7 (a) Transversal distributions of the relative intensity of the guided molecular beam at two 10 mm-spaced axial positions. (b) Dependence of the beam divergent angle on the guiding voltage.

50 Pa and a guiding voltage of ± 4 kV, which is shown in Fig. 8. We find from comparison with Fig. 2 in ref. 28 that our experimental result is very similar to that of Softley's group,²⁸ and only their most probable translational energy (~ 1.8 K) is slightly lower than ours (~ 2.3 K).

Finally, compared with the work and results of other groups,^{11,26–28} there are some new findings and results in this paper, such as (1) we use a new method, the “photoionization time-of-flight mass-spectrometer” (PI-TOF-MS) method to measure the transverse and longitudinal velocity distributions of output cold molecular beam. It should be noted that the QMS method cannot be used to conveniently measure the transverse velocity distribution of the output molecular beam and its divergent angle. (2) We experimentally study the dependences of the transverse and longitudinal temperatures on the guiding voltage, and find a new scaling law: $T_z, T_\rho \propto V_{\text{guide}}$, and experimentally verify another scaling law: $\eta \propto V_{\text{guide}}^2$.²⁶ (3) We perform Monte-Carlo simulations for the dynamic process of the molecular bent guiding, and obtain some simulated results consistent with our experimental ones. (4) By using the Monte-Carlo method, we also theoretically verify the above two scaling laws. (5) We first measure a divergent angle of the output cold molecular beam and study its dependence on the guiding voltage, and find that the divergent angle decreases exponentially with increasing

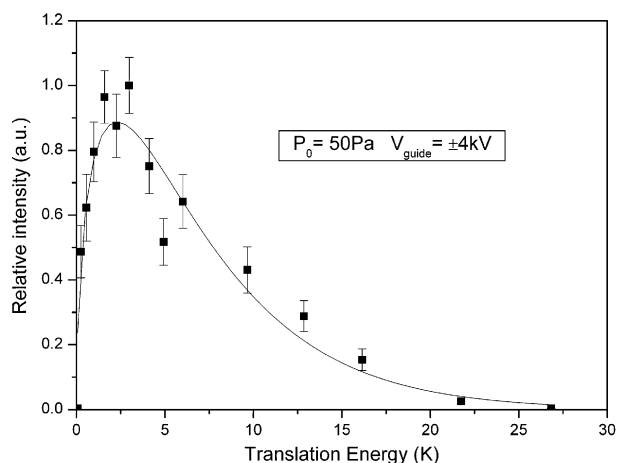


Fig. 8 Kinetic energy distribution for the guided CH_3CN beam at a gas-source pressure of 50 Pa and a guiding voltage of ± 4 kV. The squares with an error bar are the experimental data and the solid line is the fitted curve.

guiding voltage at lower guiding voltages, and tends to be a constant value at higher voltages.

5. Conclusion

In this paper, we have used the bent quadrupole electrostatic field to generate a cw cold methyl-cyanide (CH_3CN) molecular beam, and measured the longitudinal and transversal velocity distributions of the guided CH_3CN beam as well as its divergent angle, and studied the dependences of the longitudinal and transversal temperatures of the guided CH_3CN beam and the guiding efficiency on the guiding voltage, as well as the dependence of the beam divergent angle on the guiding voltage. We have also performed Monte-Carlo simulation for dynamic process of the bent guiding of cold CH_3CN beam and obtained some simulated results consistent with our experimental ones. Our study shows that our bent quadrupole electrostatic guiding scheme can be used to produce a cw cold (CH_3CN) molecular beam with a longitudinal temperature of ~ 500 mK and a transverse temperature of ~ 40 mK as the initial temperature of the incident molecular beam is 300 K and the guiding voltage is 1 kV.

In addition, the temperature of the guided molecular beam and its output flux can be easily controlled by adjusting the guiding voltage (in fact, also including the reservoir pressure). In particular, we have found a new scaling laws: the longitudinal and transversal temperatures (T_z, T_ρ) of the guided CH_3CN beam are proportional to the guiding voltage (i.e., $T_z, T_\rho \propto V_{\text{guide}}$), and further confirmed that the corresponding molecular guiding efficiency η is proportional to square of the guiding voltage ($\eta \propto V_{\text{guide}}^2$). We have also found that the divergent angle of the output CH_3CN beam will be reduced from about 19.5° to 16.2° as the guiding voltage is increased from 2 kV to 6 kV. If an ideal effusive molecular beam with a temperature of 5–10 K pre-cooled by ^4He buffer gas cooling^{29–31} is used, we could obtain a colder CH_3CN beam with a longitudinal temperature of lower than ~ 10 mK. Therefore, such a cold molecular beam has many important

applications in the fields of cold molecular physics, physics chemistry and chemical physics, *etc.*, such as the fact it cannot only be used to load a typical electrostatic or optical trap for further cooling and manipulation, but also have some important applications in the fields of cold molecular physics and molecule optics (including integrated molecule optics), cold molecular spectroscopy,² cold molecular collisions and cold chemistry,^{8,32} quantum computing and quantum information processing,⁶ and so on.

Acknowledgements

This work is supported by the National Natural Science Foundation of China under Grant Nos. 10434060, 10674047 and 10804031, the National Key Basic Research and Development Program of China under grant No. 2006CB921604, the Basic Key Program of Shanghai Municipality under Grant No. 07JC14017, the Program for Changjiang Scholar and Innovative Research Team, and Shanghai Leading Academic Discipline Project under Grant No. B408.

References

- 1 *Faraday Discussion 142: Cold and Ultracold Molecules*, 2009, the first paper of which is: D. Herschbach, *Faraday Discuss.*, 2009, **142**, 9; L. Carr, D. DeMille, R. V. Krems and J. Ye, *New J. Phys.*, 2009, **11**, 055049.
- 2 J. van Veldhoven, J. Kupper, H. L. Bethlem, B. Sartakov, A. J. A. van Rooij and G. Meijer, *Eur. Phys. J. D*, 2004, **31**, 337–349.
- 3 D. DeMille, F. Bay, S. Bickman, D. Kawall, D. Krause, Jr, S. E. Maxwell and L. R. Hunter, *Phys. Rev. A: At., Mol., Opt. Phys.*, 2000, **61**, 052507; J. J. Hudson, B. E. Sauer, M. R. Tarbutt and E. A. Hinds, *Phys. Rev. Lett.*, 2002, **89**, 023003.
- 4 Eric R. Hudson, H. J. Lewandowski, Brian C. Sawyer and Jun Ye, *Phys. Rev. Lett.*, 2006, **96**, 143004.
- 5 H. L. Bethlem, M. Kajita, B. Sartakov, G. Meijer and W. Ubachs, *Eur. Phys. J. Spec. Top.*, 2008, **163**, 55–69.
- 6 D. DeMille, *Phys. Rev. Lett.*, 2002, **88**, 067901; A. Micheli, G. Brennen and P. Zoller, *Nat. Phys.*, 2006, **2**, 341; A. André, D. DeMille, J. M. Doyle, M. D. Lukin, S. E. Maxwell, P. Rabl, R. J. Schoelkopf and P. Zoller, *Nat. Phys.*, 2006, **2**, 636.
- 7 Benjamin L. Lev, Edmund R. Meyer, Eric R. Hudson, Brian C. Sawyer, John L. Bohn and Jun Ye, *Phys. Rev. A: At., Mol., Opt. Phys.*, 2006, **74**, 061402; A. Avdeenkov and J. Bohn, *Phys. Rev. A: At., Mol., Opt. Phys.*, 2002, **66**, 052718.
- 8 R. V. Krems, *Phys. Chem. Chem. Phys.*, 2008, **10**, 4079; Stefan Willitsch, Martin T. Bell, Alexander D. Gingell, Simon R. Procter and Timothy P. Softley, *Phys. Rev. Lett.*, 2008, **100**, 043203; N. Balakrishnan and A. Dalgarno, *Chem. Phys. Lett.*, 2001, **341**, 652.
- 9 M. Gupta and D. Herschbach, *J. Phys. Chem. A*, 2001, **105**, 1626.
- 10 H. L. Bethlem, G. Berden and G. Meijer, *Phys. Rev. Lett.*, 1999, **83**, 1558; M. R. Tarbutt, H. L. Bethlem, J. J. Hudson, V. L. Ryabov, V. A. Ryzhov, B. E. Sauer, G. Meijer and E. A. Hinds, *Phys. Rev. Lett.*, 2004, **92**, 173002; J. R. Bochinski, Eric R. Hudson, H. J. Lewandowski, G. Meijer and Jun Ye, *Phys. Rev. Lett.*, 2003, **91**, 243001.
- 11 S. A. Rangwala, T. Junglen, T. Rieger, P. W. H. Pinkse and G. Rempe, *Phys. Rev. A: At., Mol., Opt. Phys.*, 2003, **67**, 043406.
- 12 Hidenobu Tsuji, Yasumasa Okuda, Takao Sekiguchi and Hideto Kanamori, *Chem. Phys. Lett.*, 2007, **436**, 331.
- 13 Dima Egorov, Thierry Lahaye, Wieland Schollkopf, Bretislav Friedrich and John M. Doyle, *Phys. Rev. A: At., Mol., Opt. Phys.*, 2002, **66**, 043401; S. E. Maxwell, N. Barhms, R. deCarvalho, D. R. Glenn, J. S. Helton, S. V. Nguyen, D. Patterson, J. Petricka, D. DeMille and J. M. Doyle, *Phys. Rev. Lett.*, 2005, **95**, 173201.
- 14 Edvardas Narevicius, Adam Libson, Christian G. Parthey, Isaac Chavez, Julia Narevicius, Uzi Even and Mark G. Raizen, *Phys. Rev. A: At., Mol., Opt. Phys.*, 2008, **77**, 051401.
- 15 Jaime Ramirez-Serrano, Kevin E. Strecker and David W. Chandler, *Phys. Chem. Chem. Phys.*, 2006, **8**, 2985; R. Fulton, A. I. Bishop and P. F. Baker, *Phys. Rev. Lett.*, 2004, **93**, 243004; R. Fulton, A. I. Bishop, M. N. Shneider and P. F. Barker, *Nat. Phys.*, 2006, **2**, 465.
- 16 Yaling Yin, Qi Zhou, Lianzhong Deng, Yong Xia and Jianping Yin, *Opt. Express*, 2009, **17**, 10706.
- 17 Ya-Ling Yin, Yong Xia and Jian-Ping Yin, *Chin. Phys. B*, 2008, **17**, 3672, arXiv:0803.0790, 2008.
- 18 P. M. Solomon, K. B. Jefferts, A. A. Penzias and R. W. Wilson, *Astrophys. J.*, 1971, **168**, L107; A. Remijan, E. C. Sutton, L. E. Snyder, D. N. Friedel, S.-Y. Liu and C.-C. Pei, *Astrophys. J.*, 2004, **606**, 917.
- 19 J. Gadhi, A. Lahrouni, J. Legrand and J. Demaison, *J. Chim. Phys. PCB*, 1995, **92**, 1984; M. Simeckova, S. Urban, U. Fuchs, F. Lewen, G. Winnewisser, I. Morino and K. M. T. Yamada, *J. Mol. Spectrosc.*, 2004, **226**, 123.
- 20 Yong Xia, Yaling Yin, Haibo Chen, Lianzhong Deng and Jianping Yin, *Phys. Rev. Lett.*, 2008, **100**, 043003.
- 21 Yong Xia, Yaling Yin, Haibo Chen, Lianzhong Deng and Jianping Yin, *J. Chem. Phys.*, 2008, **128**, 094301.
- 22 Eric R. Hudson, Doctoral thesis, *Cold Molecule Production via Stark deceleration*, University of Colorado, 2006.
- 23 Min Yun, Yang Liu, Lianzhong Deng, Qi Zhou and Jianping Yin, *Front. Phys. China*, 2008, **3**, 19.
- 24 T. D. Hain, R. B. Moision and T. J. Curtiss, *J. Chem. Phys.*, 1999, **111**, 6797.
- 25 M. Motsch, L. D. van Buuren, C. Sommer, M. Zeppenfeld, G. Rempe and P. W. H. Pinkse, *Phys. Rev. A: At., Mol., Opt. Phys.*, 2009, **79**, 013405.
- 26 T. Junglen, T. Rieger, S. A. Rangwala, P. W. H. Pinkse and G. Rempe, *Eur. Phys. J. D*, 2004, **31**, 365.
- 27 T. Rieger, T. Junglen, S. A. Rangwala, G. Rempe and P. W. H. Pinkse, *Phys. Rev. A: At., Mol., Opt. Phys.*, 2006, **73**, 061402.
- 28 M. T. Bell, A. D. Gingell, J. Oldham, T. P. Softley and S. Willitsch, *Faraday Discuss.*, 2009, **142**, 73.
- 29 M. Motsch, C. Sommer, M. Zeppenfeld, L. D. van Buuren, P. W. H. Pinkse and G. Rempe, *New J. Phys.*, 2009, **11**, 055030.
- 30 Christian Sommer, Laurens D. van Buuren, Michael Motsch, Sebastian Pohle, Josef Bayerl, Pepijn W. H. Pinkse and Gerhard Rempe, *Faraday Discuss.*, 2009, **142**, 203; L. D. van Buuren, C. Sommer, M. Motsch, S. Pohle, M. Schenk, J. Bayerl, P. W. H. Pinkse and G. Rempe, *Phys. Rev. Lett.*, 2009, **102**, 033001.
- 31 David Patterson and John M. Doyle, *J. Chem. Phys.*, 2007, **126**, 154307.
- 32 M. T. Bell and T. P. Softley, *Mol. Phys.*, 2009, **107**, 99.